Design of Triple Band Differential Rectenna for RF Energy Harvesting

Sandhya Chandravanshi, *Student Member, IEEE,* Sanchari Sen Sarma, *and* M. Jaleel Akhtar, *Senior Member, IEEE*

***Abstract*—A triple band differential rectenna for RF energy harvesting applications is proposed in this paper. The rectenna is designed to operate in frequency bands of UMTS (2.1 GHz), lower WLAN/ Wi-Fi (2.4-2.48 GHz) and WiMAX (3.3-3.8 GHz). For designing the proposed rectenna, firstly a differentially fed multi-band slot antenna, which works as the front-end receiving unit, is designed, fabricated and tested to check its performance. It is observed that a peak antenna gain of 7 dBi, 5.5 dBi and 9.2 dBi is achieved at 2 GHz, 2.5 GHz and 3.5 GHz, respectively. In the next step, a triple band differential rectifier is designed using the Villard voltage doubler where interdigital capacitors (IDC) in lieu of lumped components are used. The full rectifier circuit comprising of the rectifying unit and impedance matching circuit is fabricated and tested to check its performance in the desired bands. The peak RF-DC conversion efficiency of 68% is obtained using 3-tone measurement. In the final stage, both antenna and the rectifier circuit are integrated through SMA connecter in order to implement the proposed rectenna. Measurement of the proposed rectenna shows an approximate maximum efficiency of 53% at 2 GHz, 31% at 2.5 GHz and 15.56% at 3.5 GHz.**

***Index Terms*—RF energy harvesting, differential rectenna, Villard voltage multiplier, IDC, differential matching.**

I. Introduction

OVER the years, researchers have tried to explore different renewable sources of energy for various applications. Among various sources, the RF energy has the advantage of availability at all time of the day and has very less dependency on the weather conditions [1-4]. Different types of single band, multiband as well as broadband rectenna have been proposed in the past [5-8]. A planar rectenna for the ISM band (2.45 GHz) has been proposed in [5] with high gain of 11.5 dBi, where it has been shown that the proposed rectenna can be used to harvest energy to turn on a LED from 2.8 m of distance. A high efficiency rectenna for harnessing energy in the 2.45 GHz frequency band has been presented in [6]. Although the gain of the proposed antenna in [6] is quite high (8.6 dBi), the rectenna is fabricated on a relatively expensive RT/Duroid 6002 substrate with a dielectric constant of 2.94 and loss tangent of 0.0012. A 2.45 GHz rectenna based on a square aperture-coupled patch antenna with dual linear, polarization has recently been proposed in [7], where a cross-shaped slot is etched on the patch surface leading to a 32.5% patch size reduction. However, the efficiency achieved for this configuration is only 38.2%. A broadband dual polarized cross dipole antenna with harmonic rejection property has been employed in [8].

A planar dual band monopole antenna for energy harvesting in the GSM bands has been presented in [9]. However, the peak-gains at the two operating bands are pretty low (1.97 dBi and 3.05 dBi) for their case. In [10], a dual band rectenna has been proposed which works in the GSM 1800 and UMTS 2100 bands. The antenna has a sufficiently high gain of 10.9 dBi and 13.3 dBi at 1.85 and 2.15 GHz, respectively owing to the use of array configuration instead of a single element. However, this makes the structure less suitable for applications which require reduced antenna footprint. A dual band rectenna operating at 2.45 and 5.8 GHz has been proposed with integrated novel CPS filters and printed dipole antenna in [11]. In [12] a triple band antenna with 4 stage of rectifier circuit working at 940MHz, 1.95GHz, and 2.44 GHz with realized gain of antenna is 0.3 dBi, 2.3dBi, 3.5 dBi respectively has been proposed. In [13] a review analysis has been performed in which various rectennas including frequency and power rectenna has been discussed. A wideband twin-loop antenna has been developed with 5.2 dBi gain. For -20 dBm input RF power 9% RF-DC conversion efficiency has been reported in [14]. However, most of the rectennas discussed above employ the conventional single input configuration with moderate gain at specified frequency points.

In recent years, the new concept of the differentially fed rectenna unit has emerged to take advantage of low common-mode noise, good harmonic suppression as well as high linearity. Differential input to the rectifiers generally results into the improvement of efficiency of the overall harvesting unit. Differentially fed rectenna units are more suitable as compared to single ended antennas for ease of integration, thus eliminating the need of additional baluns. Moreover, differentially fed antennas have reduced cross polarization levels. A differential microstrip antenna with a gain of 8.5 dBi for RF Energy harvesting applications at GSM-900 band has recently been presented [15]. A rectenna with a differentially-driven rectifier for wireless power transmission applications has been proposed in [16]. It has been observed that in comparison to a single ended microstrip patch antenna, the differential one yields larger output DC power. In [17] a differential rectifier based on resistance compression network operating at 915 MHz has been proposed. A differential CMOS rectifier circuit for UHF RFID application has been proposed in [18]. However, most of these differential rectennas have been designed for a single frequency band thus limiting their usage for multi-band applications. It has recently been shown using the conventional single port configuration that the design of RF harvesting circuit operating over multiple frequency bands is quite advantageous as the overall RF to dc efficiency can be increased under these situations by simultaneously extracting RF energy from multiple ambient sources [19-20].

This article has been accepted for publication in a future issue of this journal, but has not been fully edited. Content may change prior to final publication. Citation information: DOI 10.1109/TAP.2018.2819699, IEEE Transactions on Antennas and Propagation

From above discussion, it emerges that the multi-band rectenna system for differential configuration has not been reported earlier in literature. The multi-band differentially fed rectenna would obviously be quite useful for RF energy harvesting applications as it would possess all the advantages of a differential structure such as low common-mode noise, good harmonic suppression etc. along with other advantages such as the increased RF to dc efficiency at even low RF power level due to simultaneous extraction of RF energy from multiple ambient sources. It is mainly due to this reason that a differential rectenna working over three frequency bands is proposed in this paper. The proposed triple band rectifier circuit is quite novel as it is designed using interdigital capacitors (IDCs) in lieu of lumped capacitors in order to achieve better stability. The overall rectenna is optimized for its efficient operation at relatively low RF power level due to its multi-band operation, which makes the design quite appropriate for extracting energy from the ambient RF source.

The overall work involves design and development of a triple band differentially fed receiving antenna and a rectifier circuit operating in the UMTS (2.1 GHz), lower WLAN/Wi-Fi (2.4 GHz-2.48 GHz) and WiMAX (3.3 GHz-3.8 GHz) frequency bands. The triple band properties of the proposed antenna at the desired frequencies are achieved by etching out two square loops on the ground plane, which are connected through common small slit. The antenna is simulated using the full wave simulator, the CST Microwave Studio. The antenna is then fabricated and tested for validation. The S_{d11} characteristic of the measured antenna is compared with the simulated values, and the 2D radiation patterns are plotted. The similarity between the simulated and the test results confirms the validity of the antenna design. In the next step, the triple band differentially fed rectifier circuit is independently designed, developed and tested. The proposed rectifier circuit is designed and simulated for obtaining triple band characteristics using the Advance Design System software (ADS). For implementing the rectifier circuit, the Villard voltage doubler topology is used in which lumped capacitors have been replaced by IDCs to achieve better reliability. For the triple band operation, open stubs and radial stubs are used, where the length and number of fingers of the interdigital capacitor are also optimized using ADS. The designed rectifier circuit is finally integrated with the antenna in order to observe the behavior of the proposed differential rectenna in all the three frequency bands.

II. DESIGN AND ANALYSIS OF THE ANTENNA UNIT

A. Antenna Design

The proposed triple band differentially fed antenna is a square, electromagnetically coupled, two layer antenna. The bottom patch has the differential input/output, whereas the upper layer comprises of a copper plate that acts as a reflector for the differential antenna. The antenna is designed on a 1.6 mm thick FR4 substrate with permittivity of 4.4 and a loss tangent of 0.02. All the simulations pertaining to antenna design are performed using the full wave simulator, the CST Microwave Studio. A microstrip feed line of width 3 mm is designed on the top surface (as shown in Fig. 1(a)) while the bottom surface is

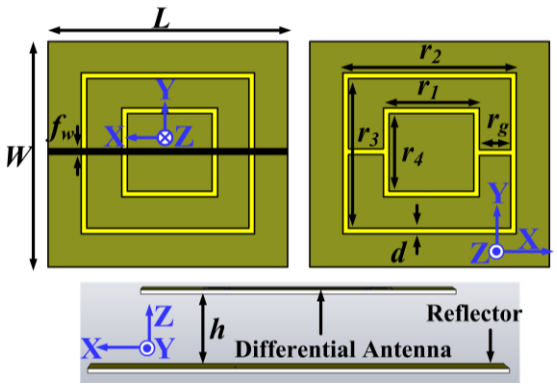

Fig. 1. Schematic of the proposed dual band differential antenna: (a) Back view, (b) Front view. (c) Side view of the proposed antenna separated from a reflector. L=120, W=120, r_1=56, r_2=72, r_3=68, r_4=52, d=2, r_g=6, f_w=3, h=28, all units are in mm.

grounded. The antenna is fed at the two ends of the microstrip line at a phase difference of 180°. Two square slots are etched out on the ground plane which is connected by a slot of length (r_g) in order to achieve the desired multi-band properties, as shown in Fig. 1(b). The differential antenna is backed by a reflector plate with spacing of 28 mm. The reflector has a dimension of 160 mm X 160 mm, which is larger than the differential antenna (120 mm X 120 mm) in order to improve the gain of the antenna and make the pattern unidirectional. The other optimized design parameters of the antenna are given in the caption of Fig. 1.

B. Analysis of the Antenna without and with the Top Reflector

In this section, the results of the differential antenna without the reflector are first discussed. The differential S_{11} or the S_{d11} characteristics of the proposed antenna is determined by the formula given below [21 - 23]:

$$S_{d11} = \frac{1}{2}(S_{11} - S_{21} - S_{12} + S_{22}) \qquad \textbf{(1)}$$

The overall design methodology of the proposed multi-band differential antenna can be explained in a step-by-step manner with the help of Fig. 2 (a) along with their respective differential reflection coefficients S_{d11} shown in Fig. 2(b). The Ant. 1 in Fig. 2(a) corresponding to inner smaller loop slit of Fig. 1(b) resonates individually at 3.8 GHz with no other resonances observed in the specified frequency range as shown in Fig. 2(b). The primary resonance of Ant 2 in Fig. 2(a) corresponding to outer loop slit of Fig. 1(b) appears at 2.8 GHz with a very weak resonance appearing near 1.9 GHz. The main reason for appearance of a minor resonance near 1.9 GHz corresponding to Ant 2 is due to weak coupling between the outer loop and the outermost patch geometry. This kind of phenomenon is not observed for the Ant 1 corresponding to inner loop due to the larger spacing between the inner loop slit and the outer patch geometry. Another higher order resonance of Ant. 2 appears close to 3.75 GHz as shown in Fig. 2(b), which might be due to second order harmonic corresponding to the weak resonance appearing near 1.9 GHz. The higher order mode of Ant. 2 near 3.75 GHz is mainly considered here due to the fact that the gain

This article has been accepted for publication in a future issue of this journal, but has not been fully edited. Content may change prior to final publication. Citation information: DOI 10.1109/TAP.2018.2819699, IEEE Transactions on Antennas and Propagation

obtained at this frequency is quite high as shown in the later part of this text. Now, in order to obtain desired operating bands, the outer and inner loop slits combined over a single ground plane are connected by a slot of length (r_g), denoted as Ant 3 in Fig. 2(a). A differential feed line of 3 mm width appears at the front side of the structure. This kind of topology by combining inner and outer loop slits through a slot results into three antenna resonances observed at 2.0 GHz, 2.55 GHz and 3.48 GHz. The two resonances appearing at 2 GHz and 2.55 GHz in this case mainly correspond to the outer loop slit, where the earlier resonance appearing at 2.8 GHz is shifted to lower frequency of 2.55 GHz. However, the third resonance appearing at 3.48 GHz is due to combination of both the loops as the resonance at 3.8 GHz corresponding to the inner loop of the antenna is merged together with the resonance appearing near 3.75 GHz corresponding to the outer loop. After merger of these two resonances, the resonant frequency of the resultant structure is shifted to 3.48 GHz due to the presence of a slot of length r_g connecting the two loops. It is observed that the value of third resonant frequency of the designed antenna can be adjusted by changing the length of the slots (r_g) connecting the inner and outer loops on both sides as shown in Fig. 1(b). The Ant. 4 in Fig. 2(a) shows the complete antenna structure, where a reflector is included at the back side (towards feed line region) at a separation of 28 mm from the antenna. The final structure of Ant. 4 shows three distinct bands at 2 GHz, 2.49 GHz, and 3.4 GHz as shown in Fig. 2(b). It is interesting to note from Fig. 2(b) that the inclusion of reflector at the back side of the antenna results into improvement of all the resonances with a slight shift in the frequency corresponding to each resonance.

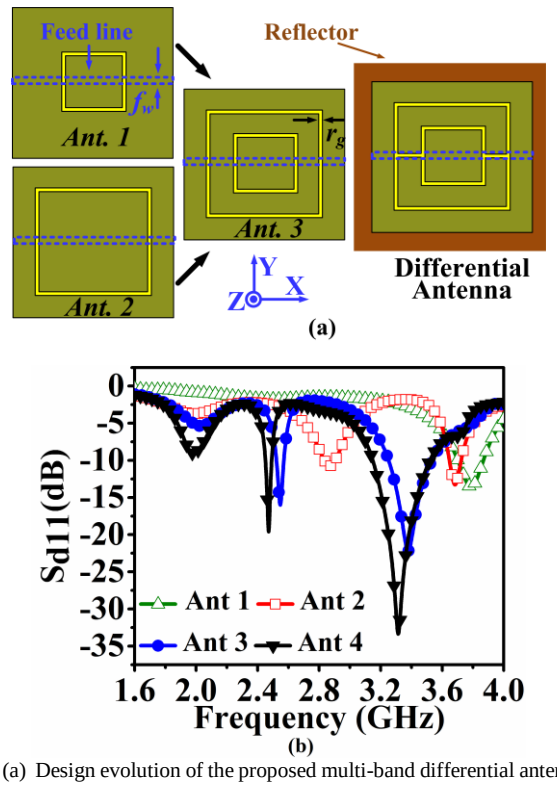

Fig. 2. (a) Design evolution of the proposed multi-band differential antenna (b) Simulated differential reflection coefficients of various antennas involved in Fig. 2 (a).

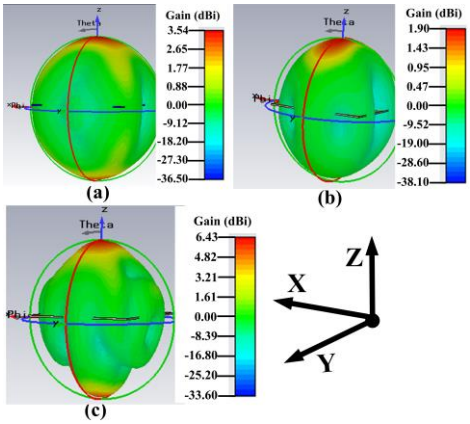

Fig. 3. The simulated 3D radiation pattern along with gain for the differential antenna without the reflector at (a) 2.0 GHz, (b) 2.55 GHz, (c) 3.48 GHz.

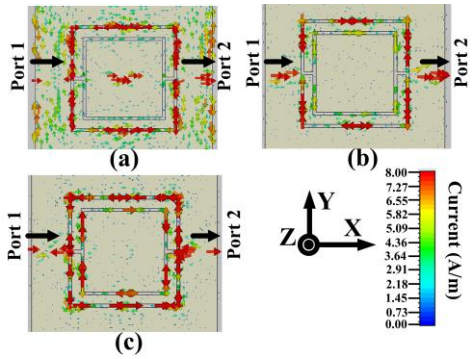

Fig. 4. Current distributions on the connected slot-rings of the antenna with the upper reflector at (a) 2.0 GHz, (b) 2.49 GHz, (c) 3.4 GHz. Where the black arrow is indicting the direction of current flow from the ports.

Figs. 3 (a), (b) and (c) show the simulated 3D radiation plots and the gain of the proposed antenna without reflector at 2 GHz, 2.55 GHz and 3.48 GHz, respectively. The corresponding gains at those frequencies are 3.54 dBi, 1.9 dBi and 6.43 dBi respectively. It can be observed from the gain plots that the maximum radiation is obtained along the z = 0 axis in both + and – z directions. Moreover, the gain at the three working bands (2 GHz, 2.49 GHz and 3.4 GHz) is not adequate to harvest energy from ambient, and hence further improvement of gain is required. Hence, a reflector plate at the back of the antenna is utilized which improves the gain, and also makes the radiation pattern uni-directional.

To further investigate the operating frequency characteristics, the current distribution on the proposed antenna at all three frequencies is plotted as shown in Fig 4. Fig 4(a) depicts that at 2 GHz most of the current exists between the outer loop and the outermost patch geometry. At 2.49 GHz, the current density is mostly concentrated at the periphery of the outer slot as shown in Fig. 4(b). On the other hand, the radiation at 3.4 GHz primarily corresponds to the combination of outer and inner slots. The current distribution is concentrated to both inner and outer loops for the 3.4 GHz of frequency as shown in Fig. 4(c). From this figure, it can also be observed that two ports are driving equal magnitude of the current with 180^0 phase difference indicating the differential feed arrangement. It is also to be noted that both the slot-rings interact to produce the multi-band operation.

This article has been accepted for publication in a future issue of this journal, but has not been fully edited. Content may change prior to final publication. Citation information: DOI 10.1109/TAP.2018.2819699, IEEE Transactions on Antennas and Propagation

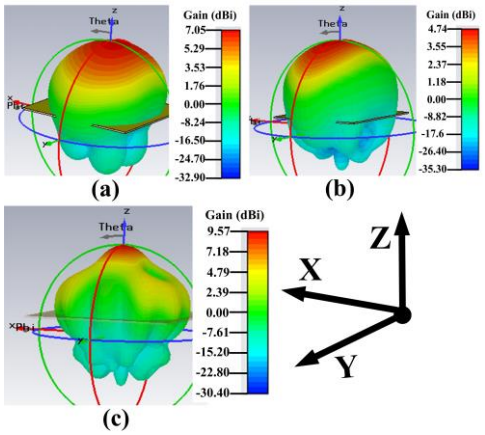

Fig. 5. The gain for the differential antenna with the upper reflector and simulated 3D radiation patterns at (a) 2 GHz, (b) 2.49 GHz, (c) 3.4 GHz.

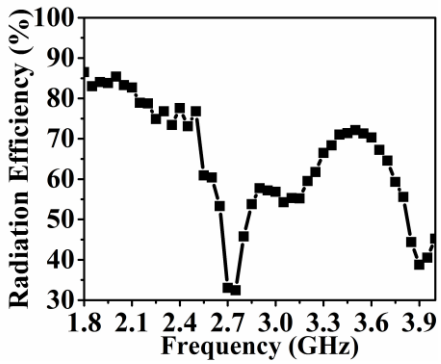

Fig. 6. Simulated radiation efficiency of the antenna.

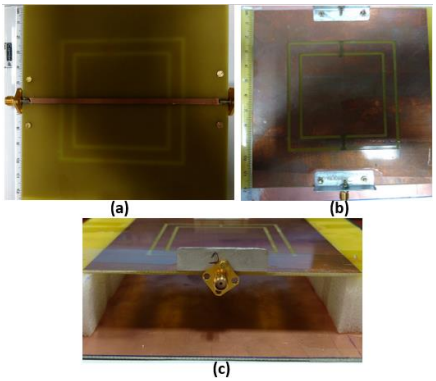

Fig. 7. Photograph of the fabricated structure: (a) Back view. (b) Front view. (c) Side view of the antenna separated by a reflector.

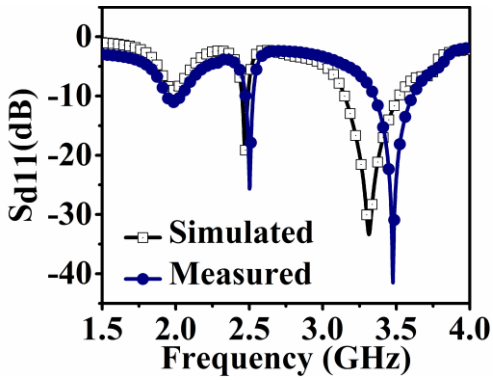

Fig. 8. Comparison of the variation of S_{d11} with frequency between the simulated and the measured design.

Fig. 6 shows the simulated radiation efficiency of the proposed triple band differential antenna. At 2 GHz, the antenna exhibits 85 % of efficiency while at 2.49 GHz and 3.4 GHz the antenna possesses 75% and 72% of efficiency, respectively.

C. Experimental Results of Antenna

Fig. 7 illustrates the fabricated prototype of the fabricated antenna. The bottom antenna is separated from the top reflector by using foam of thickness 28 mm, as shown in Fig. 7 (c). The comparison between the simulated and measured differential reflection coefficient S_{d11} of the antenna is shown in Fig. 8. Three distinct bands at 2 GHz, 2.5 GHz and 3.5 GHz can be observed from the measurement, which serve the objective of encompassing the ambient RF sources. There is a minor shift between simulated and measured results which can be attributed to the fabrication error.

Fig. 9 denotes the comparison between the simulated and measured normalized radiation plots at the two principal planes, E-plane (φ = 0°, XZ plane) and H-plane (φ = 90°, YZ plane) at 2 GHz, 2.5 GHz and 3.5 GHz of the proposed antenna. A wideband out-of-phase 180° hybrid coupler between two ports of the antenna has been used to measure the radiation patterns of the differentially driven antenna. In both planes, the cross level for the simulated and measured data is lower than -20 dB at all three frequencies which shows the differential nature of the antenna. It can be seen from the radiation patterns that the proposed antenna depicts broadside radiation along the +z direction. There is a minor disagreement between the simulated and the measured results which can be attributed to the 180° power divider not being perfect. For obtaining the uni-directional radiation pattern the electrical dimensions of the reflector is supposed to be considerably large. This criteria is better matched at the higher frequency range in this case. Since the dimension of reflector is taken to be same for all three operating frequencies, at 2 GHz (as shown in the Fig. 9(a)) the back lobe level radiation is higher as compared to the simulated one. In the same way, it can also be noticed from Fig.9 that better front-to-back ratio (FTBR) is obtained at the higher frequencies. The side lobe level is -10 dB down in case of 3.5 GHz (shown in the Fig. 9(c)), which is a considerable value. The measured gain of antenna at 2 GHz, 2.5 GHz and 3.5 GHz of frequencies are 7 dBi, 5.5 dBi and 9.2 dBi, respectively.

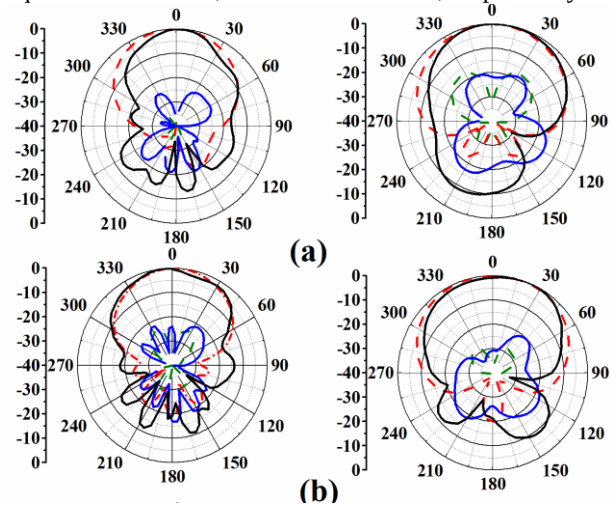

This article has been accepted for publication in a future issue of this journal, but has not been fully edited. Content may change prior to final publication. Citation information: DOI 10.1109/TAP.2018.2819699, IEEE Transactions on Antennas and Propagation

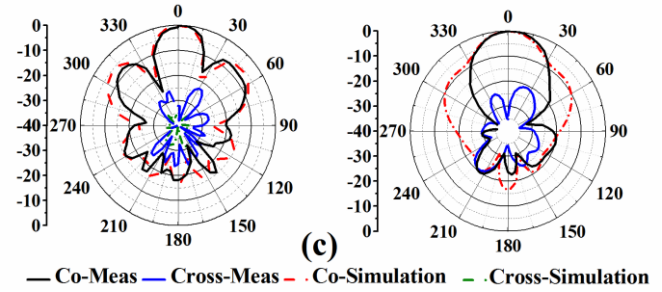

Fig. 9. Comparison between the simulated and measured 2D radiation patterns for XZ plane (Left) and YZ plane (Right) at (a) 2 GHz, (b) 2.5 GHz, (c) at 3.5 GHz.

III. RECTIFIER CIRCUIT

For the realization of differential rectenna the differential rectifier circuit including matching unit is fabricated over the low cost FR-4 substrate (ε_r = 4.4 and tanδ = 0.02). The single stage voltage doubler topology is used for the rectifier circuit consisting of the schottky diode HSMS-285C packaged with SOT-323. The circuit is simulated using the Agilent Advanced Design System (ADS) software for optimization of various parameters before its final implementation. Before the Villard voltage doubler, the triple band matching circuit is implemented by the open, short and radial stubs as shown in Fig. 10 and 11. The present differential circuit becomes more complicated because of triple band configuration. The detailed step by step design procedure of matching unit is shown in Fig. 10. Here, firstly a conventional single port rectifier circuit designated as rectifier 1 is designed as shown in Fig. 10 (a). The single port circuit works for all three operating frequencies 2 GHz, 2.5 GHz and 3.5 GHz. The designed matching unit comprises of meander line, open stubs, dual radial stub and simple radial stub. Now, in order to design the differential rectifier circuit for the three bands, replica of the same matching unit is included at the second port as depicted in Fig. 10 (b). It can be clearly observed that the configuration shown in Fig. 10 (b) designated as rectifier 2 is primarily a symmetrical differential rectifier circuit. However, the overall dimension of the designed circuit including rectifier circuit at this stage is 22 cm x 20 cm, which is very large and is not suitable as a compact harvester. Hence, it is tried to further optimize the matching circuit of rectifier 2 in order to realize a compact triple band differential rectifier circuit by shortening the overall length. It should be noted that it is usually quite difficult to optimize various parameters of the triple band differential matching circuit so that the RF-DC conversion efficiency is equally increased at all the operating frequency points. In the present situation, various parameters of each matching unit such as number of stubs, dimensions of various stubs and length of transmission line between individual components are optimized in order to realize a compact size triple band differential rectifier circuit designated as rectifier 3 as depicted in Fig. 10 (c). The optimization procedure is carried out in such a way that the input impedance of overall circuit does not change by retaining its differential nature, and the maximum possible efficiency is attained for all three operating frequencies.

In order to verify the performance of all three rectifier circuits, firstly the reflection characteristics of circuits are analyzed. As shown in Fig 10 (d), the bandwidth of rectifier 3 is more as compared to that of the rectifier 1 and 2. The efficiency for all three aforementioned rectifiers with respect to the load resistance and different input RF powers (- 2 dBm and -4 dBm) for 2 GHz is plotted in Fig. 10 (e). It can be easily observed from this figure that the efficiency of optimized circuit, rectifier 3 is higher than rectifiers 1 and 2 in the highlighted region corresponding to lower load resistance values. The final layout of the proposed rectifier circuit is shown in Fig. 11, where both the ports are connected at opposite sides of the substrate for good isolation between the ports. The inter-digital capacitors in lieu of lumped capacitors (C1 and C2) are used in the proposed rectifier in order to reduce soldering effects which enhances the overall reliability of the circuit. As shown in Fig. 11, two sources with a 180° phase difference to each other are applied to the two input ports.

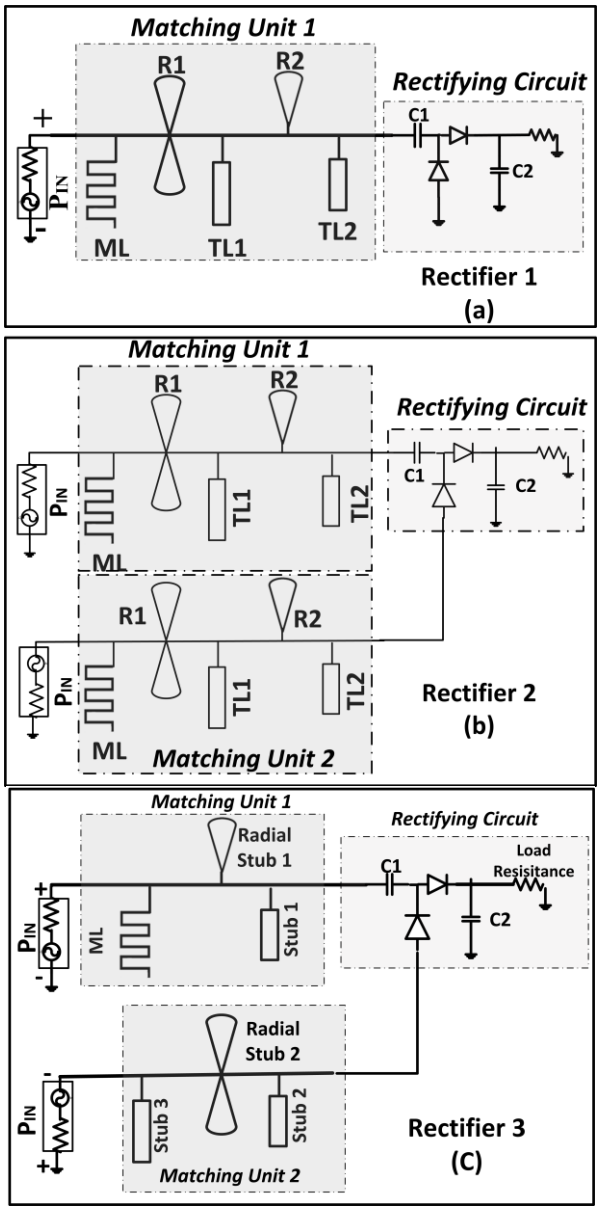

This article has been accepted for publication in a future issue of this journal, but has not been fully edited. Content may change prior to final publication. Citation information: DOI 10.1109/TAP.2018.2819699, IEEE Transactions on Antennas and Propagation

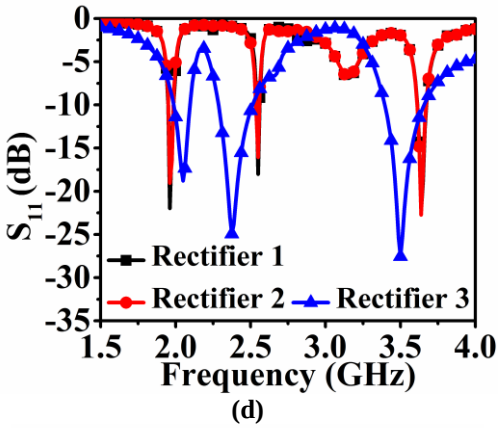

(d)

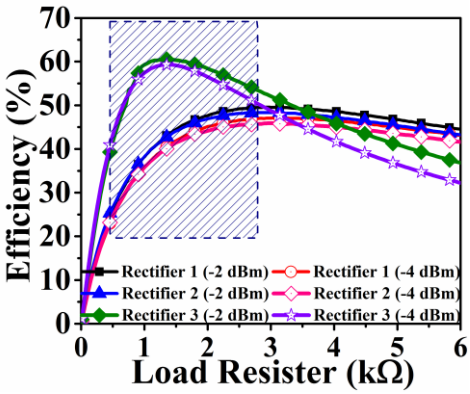

(e)

Fig. 10 (a) single port rectifier circuit (b) differentially-port rectifier circuit with symmetrical matching unit (c) optimized differential-port rectifier circuit (d) comparison of reflection coefficient (e) the simulated Efficiency of the rectifier 1, 2 and 3, with respect to the load resistance and different input RF power.

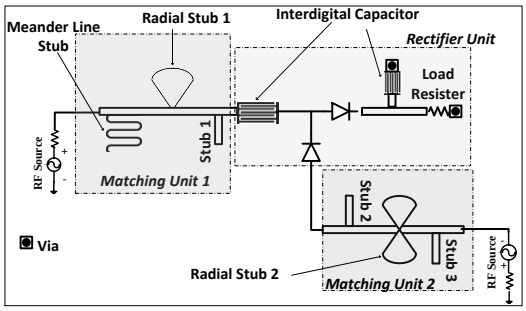

Fig. 11. Layout of proposed rectifier circuit, Stub 1= 5.8 mm, stub 2 = 14 mm, stub 3 = 4.4 mm, meander line stub = 33 mm, radial stub 1 with 70 degree and 9.4 mm radial length and radial stub 2 with 88 degree and 17.58 mm radial length.

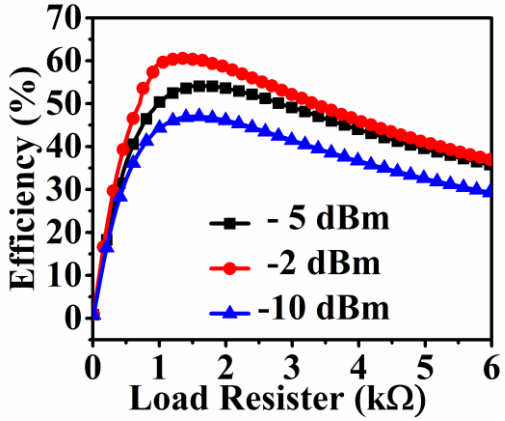

Fig. 12. Simulated efficiency for different load values at 2 GHz.

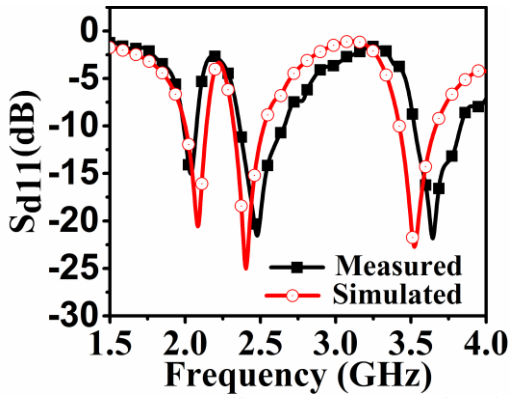

Fig. 13. Simulated and Measured differential S-parameters of rectifier circuit.

A. *Simulation Results*

The triple band differential rectifier is first simulated using the Harmonic Balance Analysis technique of Agilent ADS in order to estimate its efficiency in the desired frequency bands for different loads. It is to be noted that for computing the desired efficiency the DC voltage across the load is first determined in all the cases. The simulated efficiency at 2 GHz, is shown in Fig. 12 for varying load values at -10, -5 and -2 dBm input RF power. For this at around 1- 1.5 KΩ load values maximum efficiency is obtained. For -10 dBm and -5 dBm input RF power the optimized maximum efficiency exhibit at around 1.3 KΩ load value. However, the maximum efficiency for -2 dBm input RF power is exhibiting in the vicinity of 1.1 KΩ load value. The optimized load value is chosen to be 1.1 KΩ in order to design the circuit for maximum efficiency achievable in the low RF power range. Moreover, it can be noted form Fig. 12 that for a wide range of load values from 1 KΩ to 2 KΩ a small change in efficiency occurs. That shows, the rectifier circuit is less sensitive in this range of load values, and suitable for RF energy harvesting application.

B. *Measured Results*

The S-parameter measurements are carried out using VNA (Agilent-N5230C), and the differential S_{d11} is calculated using eq. (1). The measurements were done for the 0 dBm input power. Three distinct bands are observed at frequencies 2 GHz (with band 1.99 GHz to 2.08GHz), 2.47 GHz (with band 2.36 GHz to 2.65 GHz) and 3.6 GHz (with band 3.5 GHz to 3.8 GHZ). The rectifier circuit was also simulated using the ADS in order to extract the S-parameters to compare with the measured data. As shown in Fig. 13 there is a slight difference in simulated and measured results which can be attributed to the fabrication tolerance.

Afterwards, choosing the 1.1 KΩ load, the efficiency for all the aforementioned bands using single tone (2 GHz), 2-tone (considering 2 GHz and 2.5 GHz frequency of operation) and 3-tone (taking 2 GHz, 2.5 GHz and 3.5 GHz frequency all together) methods have been extracted as shown in Fig. 14. It can be observed from this figure that in simulation the maximum efficiency up to the 70 % can be obtained using 3-tone method at -2 dBm input power based on previously shown Fig. 10. For measurement, the input RF power is supplied from a Signal generator and its value is varied from -20 dBm to + 20 dBm. The input ports of rectifier circuit are connected using a

This article has been accepted for publication in a future issue of this journal, but has not been fully edited. Content may change prior to final publication. Citation information: DOI 10.1109/TAP.2018.2819699, IEEE Transactions on Antennas and Propagation

180° phase shifter to the signal generator. All the losses have been considered during measurements. The corresponding voltages are measured using a digital multimeter across the 1.1 KΩ resistor, from which the RF to DC conversion efficiency is calculated using the following formula.

$$\text{Efficiency}\,(\%) = \frac{V_{DC}^2 / R_L}{P_{IN}} \times 100 \qquad (2)$$

where V_{DC} is obtained DC voltage at the load resistor R_L, and P_{IN} is the available RF power in mW at an input port of the circuit. The corresponding conversion efficiency is plotted in Fig. 14. It can be observed that a peak efficiency of 68% is achieved for 3 tone measurement at an input power of -7 dBm. It can also be observed that using single source at 2 GHz, the maximum efficiency of 64 % and by using two source the 64.1 % efficiency can be obtained. There is slight difference between the simulation and measurement results that can be attributed to mismatch and insertion loss of various power combiners and 180° hybrid coupler which have been used during measurement. It is to be noted that for the simulation, signals of various tones can directly be selected and hence various individual RF components such as power combiners and 180° hybrid coupler are not required.

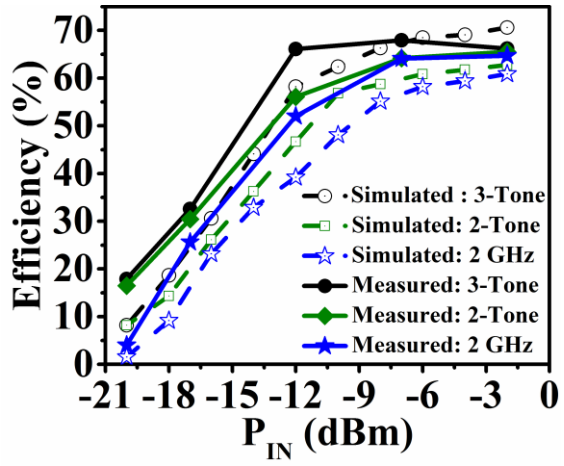

Fig. 14. Measured efficiency with respect to the input applied at each port of differential rectifier.

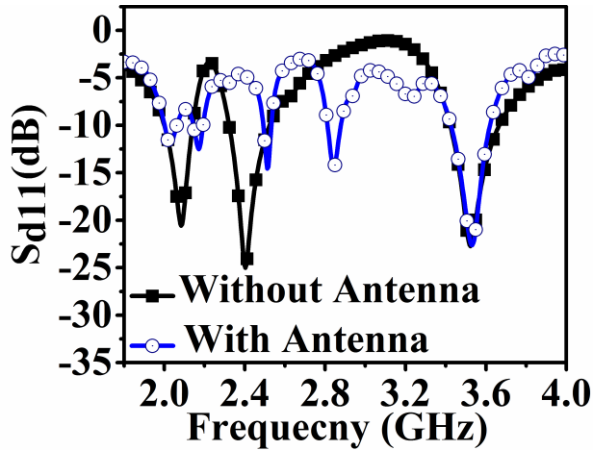

Fig. 15. Simulated S-parameters for Rectenna and rectifier circuit.

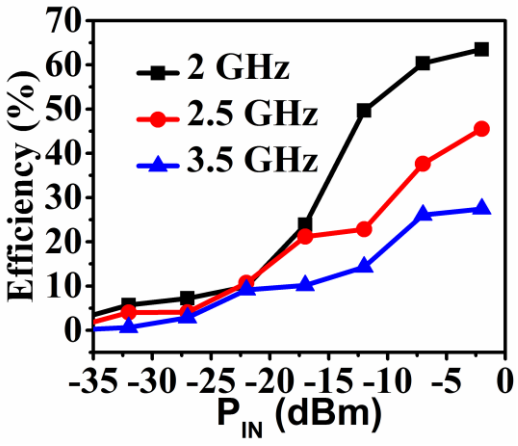

Fig. 16. Simulated efficiency of rectenna with input RF power.

IV. RECTENNA

After optimization of antenna and rectifier circuit the complete rectenna structure is simulated and fabricated.

A. Simulation Results

As the rectifier circuit and antenna characteristics are frequency dependent, hence before fabrication the co-simulation of antenna and rectifier circuit is important [24]. The impedance of antenna could be embedded in the rectifier circuit with the help of S2P file using ADS. Fig. 15 shows reflection coefficient of the antenna embedded rectifier circuit, and the rectifier circuit without antenna. From Fig. 15, some minor shift in the scattering data can be observed which might be due to slight mismatch between the antenna and the rectifier circuit.

B. Measurement Results

Fig. 16 shows simulated efficiency of the antenna embedded rectifier circuit for all frequency bands by varying the input RF power at the rectifier circuit. It can be observed from this figure that the efficiency is increasing as the input power is increased. The rectenna measurement system is shown in Fig 17. A standard horn antenna of size 244 × 164 × 204 mm^3 was used for transmitting power at desired bands of frequency. The LB-101180 horn antenna has varying gain from 6 to 16 dBi in 1 to 18 GHz range of frequency. A 6 m long cable connects the signal generator to the transmitting horn antenna, which has approximately 4.5 dB loss and the receiving antenna are placed at 1.50 m of distance from the horn antenna in the anechoic chamber.

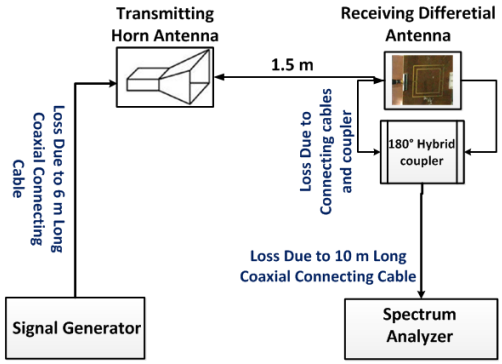

Fig. 17. Measurement setup for rectenna.

This article has been accepted for publication in a future issue of this journal, but has not been fully edited. Content may change prior to final publication. Citation information: DOI 10.1109/TAP.2018.2819699, IEEE Transactions on Antennas and Propagation

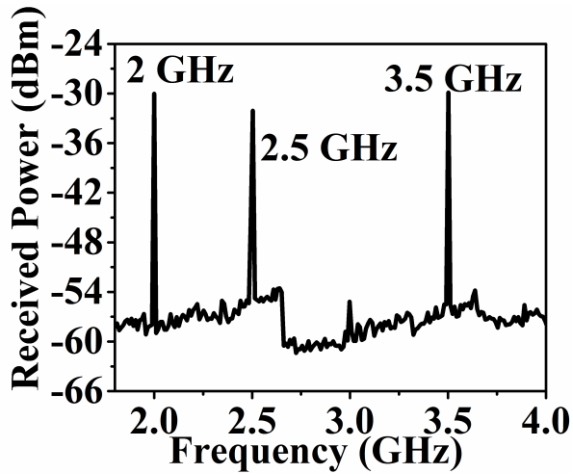

Fig. 18. Measured received power at the receiving differential antenna, when applied power to the horn antenna is 10 dBm.

The distance has been chosen so that the far field condition is valid for all three operating frequencies. The power at the receiving antenna is measured using the spectrum analyzer. The two port differential receiving antenna is connected to the spectrum analyzer via 180° hybrid coupler and a 10 m long connecting cable with approximately 7.5 dB loss. It can be noted from the Fig. 17, all the losses in between the intermediate state i.e. connecting cables and coupler has been considered for the measurements.

Fig. 18 shows received power by the receiving antenna when applied power to the horn antenna is 10 dBm. The maximum feed power to the horn antenna is 20 dBm. It can be noted that the power is mainly obtained at all three aforementioned operating frequencies. The received power measured using the standard portable spectrum analyzer is shown in Fig. 18. For this purpose, two ports of the receiving antenna are connected to the spectrum analyzer via 180° out of phase hybrid coupler in order to comply with the differential nature of received power. During measurement, the power loss due to the connecting cables and the coupler are properly accounted.

The possibility of wireless power transmission can be estimated by the link budget. For this, the corresponding transmitted power at each operating frequency is calculated in terms of the measured received power at the corresponding frequency using the standard Friis-free space transmission equation (3) shown below.

$$P_t = P_r - G_r - G_t - 20\log_{10}\left(\frac{C}{4\Pi f R}\right) \text{---} (3)$$

where P_t is the transmitted power from the horn antenna in dBm, P_r is the received power by the receiving antenna in dBm, G_r and G_t are the gain of receiving antenna and transmitting horn antenna respectively, R is the distance between horn and the receiving antenna, taken as 1.5 m, f is the operating frequency. It is to be noted that at the receiver side, all losses (coax and connectors etc.) are considered during the calculation of power. For this purpose, the laboratory setup shown in Fig. 17 is used.

The maximum RF power available from the signal generator is 20 dBm. Table 1 presents the calculated parameters of the link budget, where the EIRP is the effective isotropic radiated power. For calculation of the link budget, the gains of both transmitting horn and the receiving antenna at operating frequencies are first recorded as shown in Table 1. The output power at the receiving antenna is then measured at each operating frequency using the spectrum analyzer. The transmitted power from the horn at each operating frequency is calculated in terms of received power and gain at the corresponding frequency using the Friis formula (3). Afterwards, the output DC voltage from the rectenna is measured through multimeter at the same position for varying transmitted RF power. Fig 19(a) shows the fabricated rectifier circuit, and Fig. 19 (b) shows the measurement setup including transmitting horn antenna, rectenna and multimeter for output voltage measurement. The dc power at the rectifier output is finally determined at each operating frequency using the measured voltage as shown in last row of this table. The output DC power at the output of the rectenna can be calculated by:

TABLE 1: CALCULATED PARAMETERS OF THE LINK BUDGET

	2 GHz	2.5 GHz	3.5 GHz
Transmitter			
Transmitted Power (P_t)[dBm]	14.23	16.42	15.65
G_t [dB]	9	11	11
EIRP($P_t + G_t$)[dBm]	23.23	27.4	26.65
Receiver			
G_r [dB]	7	5.5	9.2
Propagation			
Distance (d)[m]	1.5	1.5	1.5
Free space path loss (L_f) [dB]	41.98	43.93	46.86
Received Power (P_r) [dBm]	-11.75	-11.01	-11.01
Power at the Output of Rectenna [dBm]	-15.75	-18.41	-20

$$P_{DC}\,[\text{dBm}] = 10 \text{ X } \log_{10}\left(\frac{V_{DC}^2}{R_L} \text{ X} 10^3\right) \text{----} (4)$$

For the corresponding measured value of output DC voltage (V_{DC}), the output DC power in dBm is calculated as shown in the last row of Table 1. For 2 GHz, the highest DC power is calculated to be -15.75 dBm which basically corresponds to 14.23 dBm of the transmitted power from horn. In the same way for 2.5 GHz and 3.5 GHz the dc power at the rectenna output is -18.41 dBm and -20 dBm, respectively for the highest received power at the receiving antenna.

This article has been accepted for publication in a future issue of this journal, but has not been fully edited. Content may change prior to final publication. Citation information: DOI 10.1109/TAP.2018.2819699, IEEE Transactions on Antennas and Propagation

First the output voltage has been measured by the digital multimeter across the 1.1 KΩ load resister, then DC power has been calculated which is shown in the Fig. 20. The DC power at 2 GHz is high as compare to the other two operating frequencies. The maximum obtained power is 26.58 μW at the load of the rectifier circuit while around -13 dBm RF power is fed at an input port of the rectifier circuit by receiving antenna. Fig. 21 shows the conversion efficiency characteristics of the rectenna versus input received power by the receiving antenna. It is found that the maximum efficiency of 53 % is obtained at 2 GHz of frequency while considering -13 dBm RF power at an input port of the rectifier circuit. It is to be noted that, the efficiency of 30.712 % is obtained at -12 dBm RF power at an input port of the rectifier circuit for the operating frequency of 2.5 GHz. The conversion efficiency at 3.5 GHz band is lower as compared to the other two bands due to impedance mismatch as the band covered by rectifier is somewhat shifted as compare to that of the antenna.

The overall efficiency of rectenna depends upon the performance of the antenna as well of the rectifier circuit, and that of the quality of matching between the individual antenna and the rectifier units. The efficiency of the designed antenna at the frequency of 2 GHz is highest as compared to its value at other two frequency values as seen clearly from Fig. 6. The overall efficiency of the rectenna is not same for all the three operating frequency bands. As a matter of fact, only at the lowest frequency of 2 GHz, a very good rectenna efficiency at lower input RF power level is obtained. Hence, at the upper frequency of 3.5 GHz, the low rectenna efficiency is obtained due to the lower value of the corresponding antenna efficiency at this frequency in addition to the impedance mismatch between the rectifier and the antenna units for this operating band.

As the efficiency in the present situation is mostly limited due to the low input RF power, the actual efficiency can be further increased if we can get more RF power at the receiving antenna. That can be justified using Fig. 16, where it is observed that the efficiency substantially increases for higher input power.

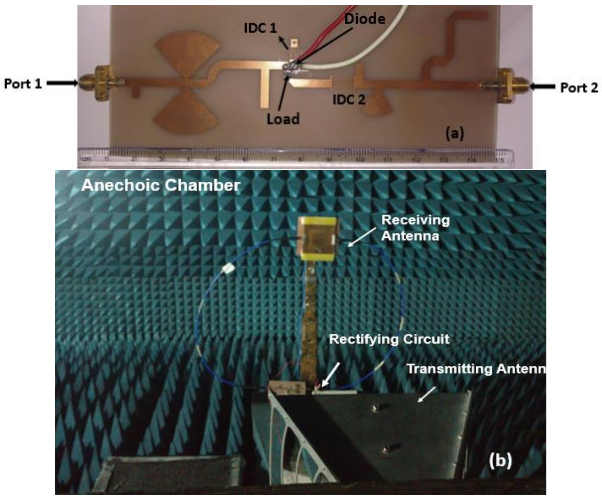

Fig. 19. (a) Fabricated Rectifier circuit (b) Measuring setup for rectenna.

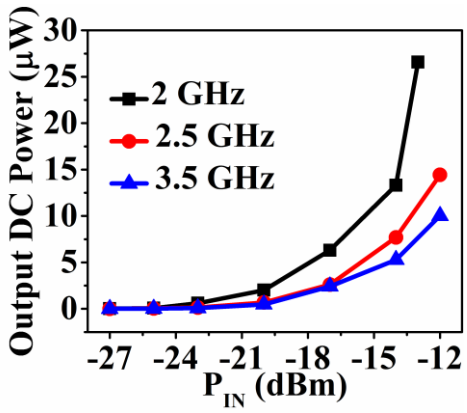

Fig. 20. Measured output DC power at the rectenna with respect to the obtained input RF power.

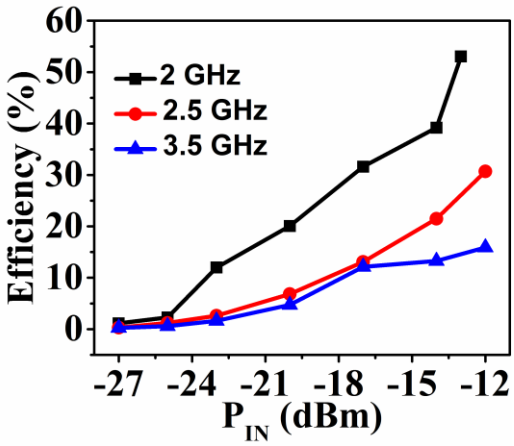

Fig. 21. Measured efficiency of rectenna with respect to obtained RF power at input of receiving antenna.

V. CONCLUSION

In this paper, a novel triple band differentially fed rectenna working in UMTS (2.1 GHz), lower WLAN/Wi-Fi (2.4 - 2.48 GHz) and WiMAX (3.3-3.8 GHz) frequencies has been proposed. The designed microstrip-fed triple band differential antenna has been realized by etching two rectangular slot-loops connected together in the ground plane. A copper patch based reflector has been used to make the radiation uni-directional possessing high peak-gain. The measured gain of antenna at 2 GHz, 2.5 GHz and 3.5 GHz of frequencies are 7 dBi, 5.5 dBi and 9.2 dBi, respectively. The triple band rectifier, along with the differential matching circuit has been independently designed, fabricated and tested to obtain the desired performance. The differential antenna has finally been integrated with the rectifier circuit to realize the proposed triple band differentially fed rectenna.

REFERENCES

[1] S. Kim, R. Vyas, J. Bito, K. Niotaki, A. Collado, A. Georgiadis, and M. M. Tentzeris, "Ambient RF energy-harvesting technologies for self-sustainable standalone wire-less sensor platforms", *Proc. IEEE,* vol. 102, no. 11, pp. 1649-1666, Nov. 2014.

[2] C. Valenta and G. Durgin, "Survey of energy-harvester conversion efficiency in far-field, wireless power transfer systems", *IEEE Microw. Mag.*, vol. 15, no. 4, pp. 108-120, June 2014.

[3] S. Kim et al., "No battery required: Perpetual RFID-enabled wireless sensors for cognitive intelligence applications", *IEEE Microw. Mag*., vol. 14, no. 5, pp. 66–77, Jul. 2013.

[4] A. Costanzo et al., "Electromagnetic energy harvesting and wireless power transmission: A unified approach", *Proc. IEEE*, vol. 102, no. 11, pp. 1692–1711, Nov. 2014.

[5] S. Cheng, C. W. Hsieh, C. H. Chang, and T. L. Jong, "Design and implementation of planer rectenna ISM-band application", *Proc. 45th European Microwave Conference*, Sep 6-11, 2015, pp. 999-1002.

[6] H. Sun, Y. X. Guo, M. He, and Z. Zhong, "Design of a high-efficiency 2.45-GHz rectenna for low-input-power energy harvesting", *IEEE Antennas Wireless Propag. Lett.*, vol. 11, pp. 929-932, 2012.

[7] A. Georgiadis, G. Vera Andia and A. Collado, "Rectenna design and optimization using reciprocity theory and harmonic balance analysis for electromagnetic (EM) energy harvesting", *IEEE Antennas Wireless Propag. Lett.* vol. 9, no. , pp. 444-446, May 2010.

[8] C. Song, Y. Houng, J. Zhou, J. Zhang, S. Yuan and P. Carter, "A high-efficiency broadband rectenna for ambient wireless energy harvesting", *IEEE Trans. Antennas Propag.*, vol. 63, no. 8, pp. 3486-3495, August 2015.

[9] Z. Zakaria, N. A. Zainuddin, M. Z. A. Abd Aziz, M. N. Husain and M. A. Mutalib, "Dual-band monopole antenna for energy harvesting system", *2013 IEEE Symposium on Wireless Technology & Applications (ISWTA)*, Kuching, Sep. 22-25, 2013, pp. 225-229.

[10] H. Sun, Y. S. Guo, M. He and Z. Zhong, "A dual-band rectenna using broadband Yagi antenna array for ambient RF power harvesting", *IEEE Antennas Wireless Propag. Lett.*, vol. 12, pp. 918-921, 2013.

[11] Y. H. Suh and K. Chang, "A high- efficiency dual- frequency rectenna for 2.45- and 5.8-GHz wireless power transmission", *IEEE Trans. Microwave Theory Tech.*, vol. 50, no.7, pp. 1784-1789, 2002.

[12] Pham, B. L. and A.-V. Pham, "Triple bands antenna and high efficiency rectifier design for RF energy harvesting at 900, 1900 and 2400 MHz", *Proc. of Int. Microwave Sympo. (IMS), WE3G-5, 2013*.

[13] N. Shinohara, "Rectennas for microwave power transmission", *IEICE Electronics Express*, vol. 10, no. 21, pp.1-13, 2013.

[14] S. Kitazawa, M. Hanazawa, S. Ano, H. Kamoda, H. Ban and K. Kobayashi, "Field test results of RF energy harvesting from cellular base station", *Proc. of 6th Global Symposium on Millimeter-Waves 2013 (GSMM2013)*.

[15] M. Arrawatia, M. S. Baghini and Girish Kumar, "Differential microstrip antenna for RF energy harvesting", *IEEE Trans. Antennas Propag.*, vol. 63, no. 4, pp. 1581-1588, April 2015.

[16] H. Sun, "An Enhanced Rectenna Using Differentially-Fed Rectifier for Wireless Power Transmission", *IEEE Antennas Wireless Propag. Lett.*, vol. 15, pp. 32-35, Apr. 2016.

[17] Q. W. Lin and X. Y. Zhang, "Differential rectifier using resistance compression network for improving efficiency over extended input power range", *IEEE Trans. Microwave Theory Tech.*, vol. 64, no. 9, pp. 2943-2954, Sept. 2016.

[18] K. Kotani, A. Sasaki and T. Ito, "High-efficiency differential-drive CMOS rectifier for UHF RFIDs", *IEEE Journal of Solid-State Circuits*, vol. 44, no.11, pp. 3011-3018, Nov. 2009.

[19] N. Shariati, W. S. T. Rowe, J. R. Scott and K. Ghorbani, "Multi-Service Highly Sensitive Rectifier for Enhanced RF Energy Scavenging", *Scientific Reports*, May 2015.

[20] J. A. Hagerty, F. B. Helmbrecht, W. H. McCalpin, R. Zane,and Z. B. Popovic, "Recycling ambient microwave energy with broad-band rectenna arrays", *IEEE Trans. Microwave Theory Tech.*, vol. 52, no. 3, pp. 1014-1024, March 2004.

[21] D. E. Bockelman and W. R. Eisenstadt, "Combined differential and common-mode scattering parameters: Theory and simulation", *IEEE Trans. Microw. Theory Tech.*, vol. 43, no.7, pp. 1530-1539, Jul. 1995.

[22] R. Meys and F. Janssens, "Measuring the impedance of balanced antennas by an S-parameter method", *IEEE Antennas and Propag. Mag*., vol. 40, no. 6, 62–65, Dec. 1998.

[23] D. E. Bockelman, and W. R. Eisenstadt, "Pure-mode network analyzer for on-wafer measurements of mixed-mode S-parameters of differential circuits", *IEEE Trans. Microw. Theory Tech.*, vol. 45, no. 7, pp. 1071-1077, Jul. 1997.

[24] X.X. Yang, C. Jiang, A. Z. Elsherbeni, F. Yang and Y. Q. Wang, "A Novel compact printed rectenna for data communication system", *IEEE Trans. Antenna Propag.*, vol. 61, no. 5, pp. 2532-2539, May 2013.